Chemical Science

ROYAL SOCIETY OF CHEMISTRY

EDGE ARTICLE

View Article Online
View Journal | View Issue

Cite this: *Chem. Sci.*, 2024, **15**, 19057

All publication charges for this article have been paid for by the Royal Society of Chemistry

Effect of cyclic topology *versus* linear terpolymers on antibacterial activity and biocompatibility: antimicrobial peptide avatars†

Md Aquib,[a] Wenting Yang,[b] Luofeng Yu,[ac] Vinod Kumar Kannaujiya,[a] Yuhao Zhang,[b] Peng Li,[c] Andrew Whittaker,[b] Changkui Fu*[b] and Cyrille Boyer*[a]

Host-defense peptides (HDPs) and their analogs hold significant potential for combating multidrug-resistant (MDR) bacterial infections. However, their clinical use has been hindered by susceptibility to proteases, high production costs, and cytotoxicity towards mammalian cells. Synthetic polymers with diverse topologies and compositions, designed to mimic HDPs, show promise for treating bacterial infections. In this study, we explored the antibacterial activity and biocompatibility of synthetic amphiphilic linear (LPs) and cyclic terpolymers (CPs) containing hydrophobic groups 2-ethylhexyl (E) and 2-phenylethyl (P) at 20% and 30% content. LPs were synthesized *via* RAFT polymerization and then cyclized into CPs through a hetero-Diels–Alder click reaction. The bioactivity of these terpolymers was correlated with their topology (LPs *vs.* CPs) and hydrophobic composition. LPs demonstrated superior antibacterial efficacy compared to CPs against four Gram-negative bacterial strains, with terpolymers containing (P) outperforming those with (E). Increasing the hydrophobicity from 20% to 30% in the terpolymers increased toxicity to both bacterial and mammalian cells. Notably, our terpolymers inhibited the MDR Gram-negative bacterial strain PA37 more effectively than gentamicin and ciprofloxacin. Furthermore, our terpolymers were able to disrupt cell membranes and rapidly eliminate Gram-negative bacteria (99.99% within 15 minutes). Interestingly, CPs exhibited higher hemocompatibility and biocompatibility with mammalian macrophage cells compared to LPs, showcasing a better safety profile (CPs > LPs). These findings underscore the importance of tailoring polymer architectures and optimizing the hydrophilic/hydrophobic balance to address challenges related to toxicity and selectivity in developing antimicrobial polymers.

Received 29th August 2024
Accepted 17th October 2024

DOI: 10.1039/d4sc05797j

rsc.li/chemical-science

Introduction

Antimicrobial resistance (AMR) is a pressing global health crisis, recognized by the World Health Organization (WHO) as one of the top 10 global health threats in 2021.[1,2] While AMR can arise naturally through bacterial evolution, the alarming increase is primarily driven by the misuse of antibiotics in humans, animals, and agriculture,[3,4] which was recently exacerbated by the COVID-19 pandemic.[5] The emergence of highly resistant strains, particularly against last-resort antibiotics, underscores the urgent need for novel therapeutic approaches.[3,6,7] A 2022 WHO report concluded that both existing and developing antibacterials are insufficient to address the growing AMR crisis.[8] Since 2017, only 12 new antibiotics have been approved,[8] and offer limited clinical advantages over existing antimicrobial therapies, with most belonging to established antibiotic classes with known resistance mechanisms.[8] Without innovative solutions, AMR infections are projected to become increasingly difficult to manage, potentially surpassing cancer as a leading cause of death by 2050.[9]

One promising solution is the development of synthetic antimicrobial polymers (APs), which are bio-inspired macromolecules that mimic host defense peptides (HDPs).[10–13] APs are designated to kill bacteria through membrane disruption, a mechanism believed to be less susceptible to resistance development.[12–17] Typically composed of cationic and hydrophobic components,[13,18] APs preferably target negatively charged bacterial cell surfaces,[19,20] while largely sparing the less negatively charged mammalian cell membranes.[11,12,19,21,22] However, the inherent presence of positive charges can lead to cytotoxicity and selectivity issues,[23] limiting their clinical applications.[24]

[a]*Cluster for Advanced Macromolecular Design (CAMD) and Australian Centre for NanoMedicine (ACN), School of Chemical Engineering, UNSW Australia, Sydney, NSW 2052, Australia*

[b]*Australian Institute for Bioengineering and Nanotechnology, The University of Queensland, St Lucia, Queensland, 4072, Australia*

[c]*Frontiers Science Center for Flexible Electronics (FSCFE), Xi'an Institute of Flexible Electronics (IFE) and Xi'an Institute of Biomedical Materials & Engineering (IBME), Northwestern Polytechnical University, 127 West Youyi Road, Xi'an 710072, China. E-mail: cboyer@unsw.edu.au; changkui.fu@uq.edu.au*

† Electronic supplementary information (ESI) available. See DOI: https://doi.org/10.1039/d4sc05797j

Therefore, a major focus in AP research is optimizing selectivity by enhancing antimicrobial activity while minimizing non-specific toxicity towards non-bacterial cells.[25,26] The antibacterial activity and biocompatibility of APs are influenced by various structural components, including the type of cationic groups, monomer sequence, molecular weight dispersity, molecular weight, chemical composition, amphiphilic balance, and topology.[13,27–32] Recent advances in polymer synthesis, particularly in reversible-deactivation radical polymerization,[33–36] have allowed researchers to fine-tune these parameters, resulting in the design of macromolecules with enhanced antimicrobial activities and superior biocompatibility.[12,37–41] Studies have highlighted the importance of polymer topologies, such as bottlebrushes,[42–44] star,[37,45–47] hyperbranched,[37,40] and cyclic architectures,[48–50] in improving the biocompatibility of APs compared to their linear counterparts.[38,51] Among the explored polymer topologies, cyclic polymers, characterized by their ring-like structures without chain ends,[52–54] have garnered sporadic interest in bioapplications.[55,56] Due to their unique topology, cyclic polymers exhibit reduced hydrodynamic size, enhanced stability, and slower degradation compared to their linear counterparts.[57,58] These structural differences also influence chain mobility, impacting self-assembly behavior in solution,[55,59] which can lead to prolonged blood circulation time, greater drug-loading capacity, and improved colloidal stability.[56,60,61] As a result, cyclic polymers are emerging as attractive materials for bioapplications,[55,56,62] especially in antibacterial contexts.[48–50]

To date, only a very limited number of studies (three, to our knowledge) have investigated the antimicrobial activity of cyclic polymers.[48–50] Among them, the work of Duan and colleagues is notable for being the only to report the preparation of cationic cyclic copolymers through the copolymerization of vinyl monomers, specifically 2-(*N*,*N*′-dimethylamino)ethyl methacrylate with a hydrophobic monomer. Their findings revealed that cyclic copolymers exhibited superior antimicrobial efficacy and lower cytotoxicity compared to their linear analogs, largely due to their compact and reduced hydrodynamic volume.[48] The Alabi's team and Verhaeghe & Bonduelle's team have reported the formation of cyclic oligothioetheramide and peptides and investigated their antimicrobial activities.[49,50]

Building on these pioneering efforts, we decided to prepare for the first time cyclic terpolymers. In this study, we leverage a combination of reversible addition–fragmentation chain transfer polymerization and hetero photo-mediated Diels–Alder click reaction, introduced by Barner–Kowollik's group,[63–67] to prepare a library of linear and cyclic amphiphilic cationic statistical terpolymers. By systematically investigating the effects of topology (linear *vs.* cyclic), compositions and hydrophobicity, we aim to elucidate the structure–activity relationships governing their antibacterial, hemolytic, and cytotoxic properties, thereby advancing the development of effective APs.

Results and discussion

Synthesis and characterization of linear and cyclic terpolymers

In this study, we utilized a reversible addition–fragmentation chain transfer (RAFT) polymerization to synthesize amphiphilic cationic statistical linear terpolymers (LP), which was further cyclized into cyclic terpolymers (CP) using hetero-Diels–Alder click reaction. RAFT polymerization was selected for its control over a wide range of monomers[28,34,37,41,68,69] and molecular weight, as well as its compatibility with light-induced Diels–Alder cyclization reactions.[63,64,70] A functional RAFT agent containing a benzaldehyde group for subsequent Diels–Alder cyclization was synthesized by reacting 2-(3-hydroxypropoxy)-6-methylbenzaldehyde (**I**) with 4-cyano-4-(phenylcarbonothioylthio)pentanoic acid (CPADB) (Fig. 1A).[64] The successful formation of the RAFT agent was confirmed by ^{1}H NMR analysis (ESI (ESI), Fig. S2†) and UV–vis spectroscopy, with the latter revealing a characteristic absorption peak at ∼310 nm attributed to the characteristic π–π* transition of the thiocarbonyl group in the RAFT agent (ESI, Fig. S3†).

Following our previous study,[37] we then utilized our prepared RAFT agent to synthesize terpolymers with a targeted degree of polymerization (X_n) of 50 (ESI, Fig. S4†). Each terpolymer maintained a constant 50% ratio of the cationic monomer *tert*-butyl (2-acrylamidoethyl) carbamate (Boc-AEAm), while varying the proportion of neutral hydrophilic monomer, polyethylene glycol methyl ether acrylate (PEGMEA) from 20% to 30%. The remaining 30% or 20% of each terpolymer consisted of one of two hydrophobic monomers: either the branched 2-ethylhexyl acrylate (E) or the aromatic 2-phenylethyl acrylate (P) (ESI, Fig. S5–S8†). The resulting polymers were purified by precipitation and divided into two batches. One batch was subjected to Diels–Alder cyclization reaction under 310 nm light, while the other batch was left unreacted. Subsequently, both LPs and CPs underwent Boc deprotection with trifluoroacetic acid (TFA) to generate primary ammonium functionalities. These terpolymers were systematically named according to their topology (LP and CP), hydrophobic monomer types (E or P), and composition (20% or 30% hydrophobic monomer). For example, a linear polymer containing 20% E monomer was designated LPE-20, while its cyclic counterpart was named CPE-20.

Synthesis and characterization of linear terpolymers

The monomer feed ratios for LPE-20, LPE-30, LPP-20, and LPP-30 were confirmed *via* ^{1}H NMR spectroscopy of crude reactions at $t = 0$ (ESI, Fig. S9 and S14†). After 30 h of polymerization at 70 °C, monomer conversions ranged between 90% and 93% (ESI, Fig. S10 and S15 and Table S1†). The resulting Boc-protected LPs (LPE-20, LPE-30, LPP-20, and LPP-30) showed minimal deviations from the initial feed ratios, as determined by ^{1}H NMR spectroscopy (ESI, Fig. S10 and S15†). Notably, ^{1}H NMR spectra of the Boc-protected LPs displayed characteristic peaks of the RAFT agent. Signals around 10.55 ppm and 2.46 ppm are attributed to CH-aldehyde group ((a) ESI, Fig. S10 and S15†) and $-CH_3$ group ((d and e) ESI, Fig. S10 and S15,† respectively) of orthoquinodimethane moiety, confirming the presence of the RAFT agent.[68,69] These Boc-protected LPs displayed well-controlled, monomodal molecular weight distributions (MWDs) with dispersity ($Đ$) values ranging from 1.16 to 1.40 (Table 1 and ESI, Fig. S19†), as determined by size exclusion chromatography (SEC). It is important to note that the

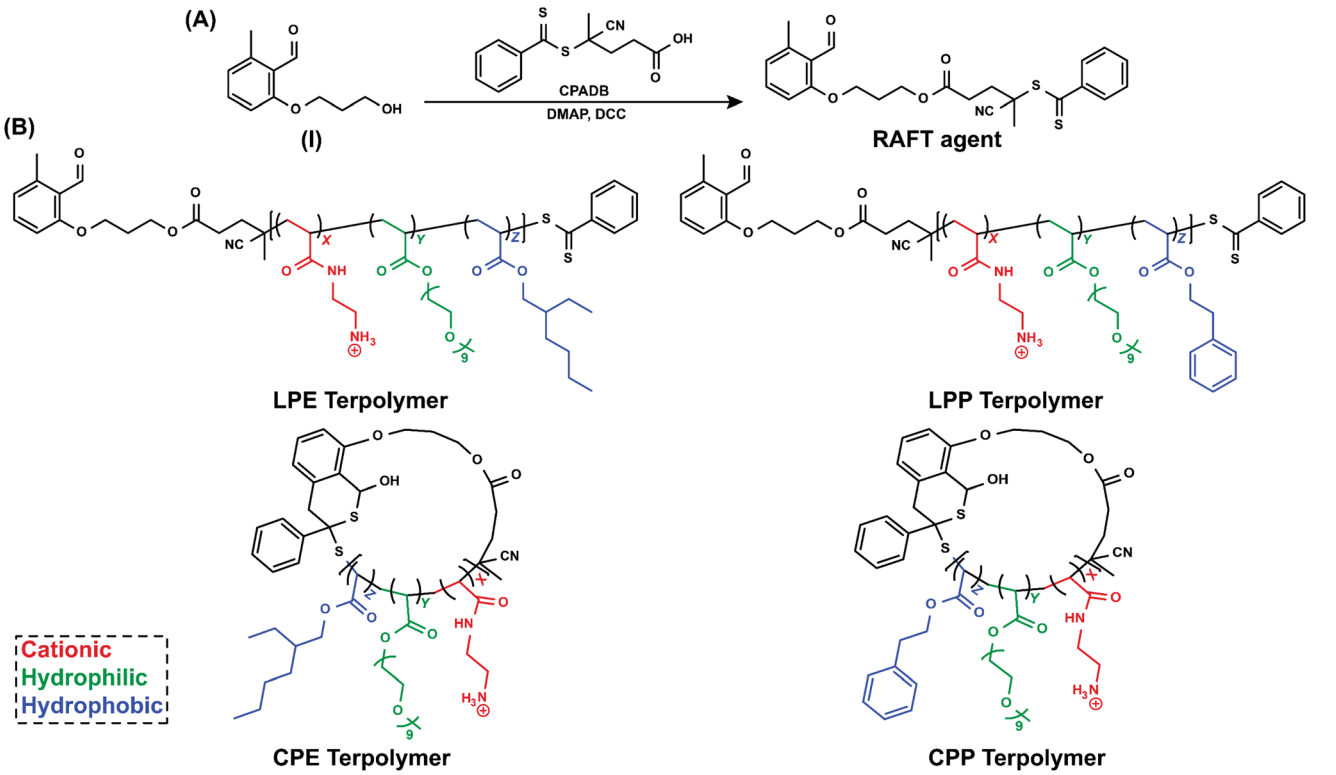

Fig. 1 (A) Synthesis scheme of RAFT agent. (B) Chemical structures of amphiphilic LPE, CPE, LPP, and CPP (*X* = percentage of cationic groups, *Y* = percentage of hydrophilic groups, and *Z* = percentage of hydrophobic groups.

experimental M_n determined by SEC deviated from the theoretical and ^{1}H NMR-calculated values (Table 1). This discrepancy was attributed to differences in hydrodynamic volume between the PMMA standards and the terpolymers, which was previously reported.[37,71] Effective removal of Boc-groups by treatment with TFA, followed by purification by precipitation, was verified by the absence of *tert*-butyl protons at $\delta = 1.45$ ppm and the presence of a free cationic primary ammonium groups at $\delta \approx 8.2$ ppm (ESI, Fig. S11 and S16†). Importantly, the characteristic peaks of the orthoquinodimethane moiety (CH-aldehyde (a) and –CH_3 (d, e)) remained visible in the ^{1}H NMR spectra of the purified terpolymers (ESI, Fig. S11 and S16†), indicating the stability of the RAFT agent post-TFA treatment. Furthermore, UV-vis spectra of the LPs (LPE-20 and LPP-30), confirmed the characteristic π–π^* absorption peak of the thiocarbonyl moiety at approximately 310 nm (Fig. 2A), thus verifying the presence of orthoquinodimethane and dithiobenzoate moieties at the two terminal ends of the terpolymers.[68,69]

Synthesis and characterization of cyclic terpolymers

The Boc-protected linear precursors were subsequently cyclized into Boc-protected CPs *via* a 310 nm light-induced Diels–Alder click reaction. To promote intramolecular cyclization over intermolecular coupling, the reaction was carried out under a highly diluted reaction condition (25 mg L^{-1}).[68] Mild UV irradiation triggered the formation of photoenol groups from the orthoquinodimethane end groups,[68,69] which then underwent Diels–Alder cycloaddition with the dithioester groups located at the opposite termini of the LPs. This reaction proceeded efficiently at room temperature in the presence of air.[68,69] Upon 12 hours of irradiation, the resulting Boc-protected CPs were readily isolated by solvent evaporation (ESI, Fig. S4†).

The success of the cyclization reaction and the formation of Boc-protected CPs were confirmed by a combination of ^{1}H-NMR, SEC, and UV-vis spectroscopy analyses. The ^{1}H-NMR spectra of the Boc-protected CPs indicated the complete disappearance of peaks at around 10.55 and 2.46 ppm (ESI, Fig. S12 and S17†), which correspond to the CH aldehyde group and methyl group of orthoquinodimethane moiety in the Boc-protected linear precursors (ESI, Fig. S10 and S15†).[68,69] While the proton signal of the newly formed isothiochroman group, expected upon successful cyclization, could not definitively be identified in the ^{1}H-NMR spectrum (ESI, Fig. S12 and S17†) due to the complexity of the terpolymer system, the absence of the orthoquinodimethane (–CH_3 and CH-aldehyde) peaks strongly supports the successful formation of cyclic structures. UV–vis spectroscopy further corroborated the successful cyclization. The characteristic absorption peak around 310 nm, associated with the dithiobenzoate moiety of the linear precursor (Fig. 2B), disappeared in the spectra of the Boc-protected CP (Fig. 2B), confirming the loss of the dithiobenzoate group upon cyclization. Furthermore, a visual change from the initial pink color of the LP to the brown color of the CP was observed after cyclization (ESI, Fig. S20A†).

Table 1 Summary of prepared polymer properties. Polymer compositions (mol%), molecular weights (M_n), dispersity ($Đ$), average hydrodynamic diameter (D_h), zeta potential (ζ), and $M_{n,cyclic}/M_{n,linear}$ ratio values were determined by ^{1}H NMR, SEC, and DLS analyses

Polymer	Feed ratio cationic : hydrophilic : hydrophobic (mol%)	Polymer composition cationic : hydrophilic : hydrophobic[a,b] (mol%)	Targeted M_n (kg mol^{-1})	M_n [a,b] (kg mol^{-1})	M_n [b,c] (kg mol^{-1})	$Đ$ [b,c]	D_h [d,e] (nm)	D_h [d,f] (nm)	ζ [d,e] (mV)	$M_{n,cyclic}/M_{n,linear}$ [b,c]
LPE-20	50 : 30 : 20	52 : 30 : 18	14.8	14.2	12.0	1.36	113.8 ± 8.2	4.3 ± 0.7	56.9 ± 2.4	0.85
CPE-20	50 : 30 : 20	52 : 30 : 18	14.8	14.2	10.2	1.41	76.1 ± 5.2	5.0 ± 0.3	49.4 ± 0.4	
LPE-30	50 : 20 : 30	52 : 20 : 28	13.3	13.5	14.5	1.16	108.8 ± 13.3	3.6 ± 0.8	61.8 ± 0.9	0.82
CPE-30	50 : 20 : 30	52 : 20 : 28	13.3	13.5	12.0	1.38	102.9 ± 7.1	5.3 ± 0.6	57.2 ± 0.2	
LPP-20	50 : 30 : 20	50 : 29 : 21	14.7	16.4	11.1	1.30	97.9 ± 7.1	4.1 ± 0.2	39.9 ± 0.1	1.0
CPP-20	50 : 30 : 20	50 : 29 : 21	14.7	16.4	11.3	1.34	88.5 ± 6.1	6.4 ± 0.4	41.6 ± 0.5	
LPP-30	50 : 20 : 30	49 : 20 : 30	13.2	13.4	11.4	1.40	119.7 ± 8.2	8.0 ± 1.4	58.7 ± 0.7	0.92
CPP-30	50 : 20 : 30	49 : 20 : 30	13.2	13.4	10.6	1.45	106.2 ± 28.6	5.3 ± 1.0	56.3 ± 0.3	

[a] Determined by ^{1}H NMR spectroscopy after polymerization (t = 30 h) (calculations available in ESI). [b] Based on Boc protected polymers. [c] Determined by SEC-DMAc analysis using poly(methyl methacrylate) (PMMA) as the standard. [d] Based on Boc deprotected terpolymers. [e] Analysis performed in Milli-Q water (DLS). [f] Analysis performed in PBS (pH 7.4; DLS). Terpolymers were synthesized with a targeted X_n of 50.

In addition, SEC analysis confirmed the successful cyclization by revealing the expected shift of MWDs to lower values for the Boc-protected CPs compared to their linear analogues (Fig. 2C and ESI, Fig. S19†). This shift, along with the observed smaller number-average molecular weight (M_n) of Boc-protected CPs compared to their linear counterparts (Table 1), is attributed to the reduced hydrodynamic volume of cyclic polymers.[68,69,72] The $M_{n,cyclic}/M_{n,linear}$ ratios in our study were calculated and found to be slightly higher than the 0.8 reported in previous publications involving the cyclization of homopolymers.[52,63,68] However, studies on cyclic copolymers have also shown $M_{n,cyclic}/M_{n,linear}$ ratios greater than 0.8, which was attributed to the specific structure of these copolymers containing different monomers.[48,50] In addition, minor coupling reactions, likely due to the complex ternary monomer system and steric hindrance from the bulky PEGMEA groups, were observed in the SEC chromatograms (Fig. 2C and ESI, Fig. S19†), resulting in a slight increase in $Đ$ (1.34 to 1.45) compared to their linear analogues (Table 1) consistent with other cyclic polymer synthesis study.[72] Finally, the successful deprotection of Boc-groups from CPs using TFA was confirmed by the absence of *tert*-butyl group at around δ = 1.45 ppm and the emergence of cationic primary ammonium groups at $\delta \approx$ 8.2 ppm (ESI, Fig. S13 and S18†).

Upon purification, the terpolymers (LPs and CPs) (ESI, Fig. S20B and C†) were dissolved in Milli-Q water and subjected to dynamic light scattering (DLS) analysis. The amphiphilic LPs exhibited average hydrodynamic diameter (D_h) values ranging from 97.9 to 119.7 nm in Milli-Q water (Table 1). In contrast, the CPs consistently displayed smaller average D_h values, ranging from 76.1 to 106.2 nm (Table 1). This reduction in D_h for CPs aligns with expectations due to their reduced hydrodynamic volume compared to linear polymers. Zeta potential (ζ) measurements for both LPs and CPs revealed positive values ranging from 39.9 to 61.8 mV in Milli-Q water, confirming the presence of cationic groups (Table 1). Additionally, the terpolymers (LPs and CPs) were assessed in PBS (pH 7.4) (Table 1 and ESI, Table S2†), where a significant decrease in both D_h and ζ was observed compared to the terpolymers analyzed in Milli-Q water (Table 1 and ESI, Table S2†), in agreement with our previous antibacterial study.[37]

Antibacterial activity

To assess the influence of topology, hydrophobic monomer type, and monomer composition on the antibacterial activity of our terpolymers, we determined the minimum inhibitory concentrations (MIC_{90}). MIC_{90} is defined as the lowest concentration of a compound required to inhibit 90% of bacterial growth by compared to untreated controls after a 20 h incubation period. We used colistin, gentamicin, and ciprofloxacin, as reference antibacterial agents (control). Four Gram-negative strains, including *Escherichia coli* (EC K12), *Pseudomonas aeruginosa* (PA, ATCC 27853; and PA37, a multidrug-resistant (MDR) strain), *Acinetobacter baumannii* (AB, ATCC 19606), and a Gram-positive strain *Staphylococcus aureus* (SA,

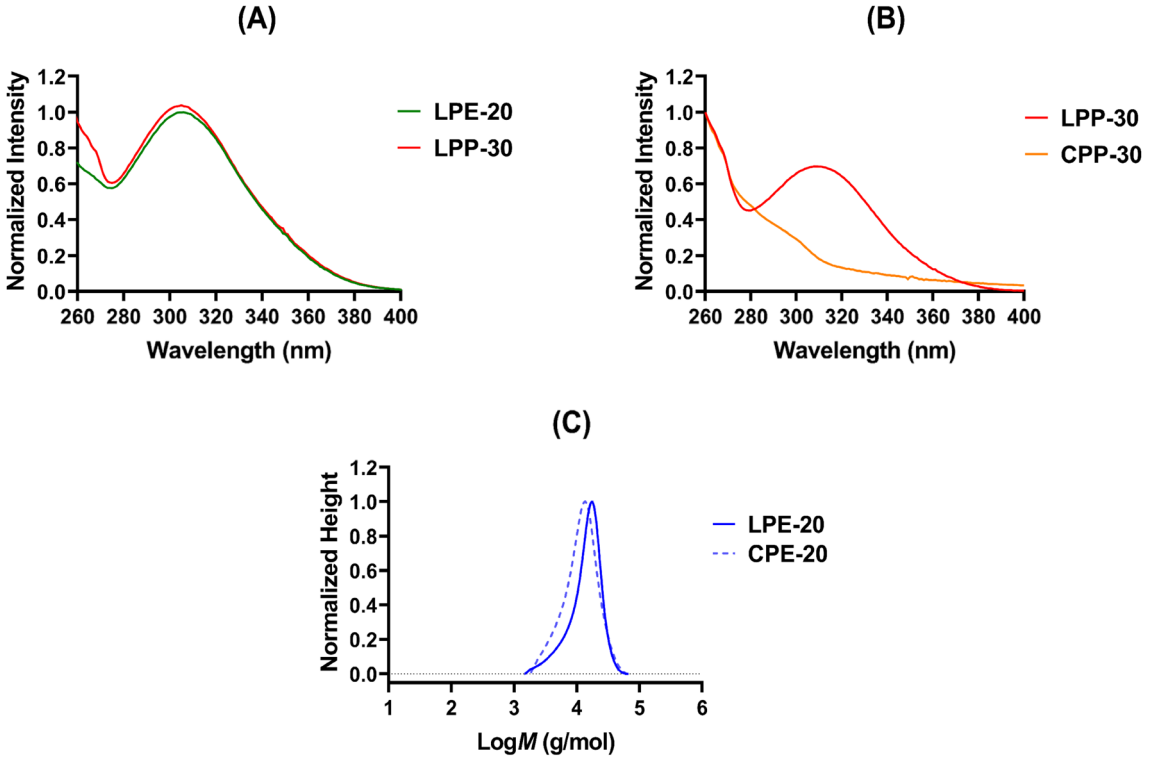

Fig. 2 (A) UV-vis spectra of LPs (LPE-20 and LPP-30) in DMSO. (B) UV-vis spectra of Boc-protected LP (LPP-30) and its corresponding CP (CPP-30) in DMSO. (C) MWDs of the Boc-protected LPE-20 and CPE-20 terpolymers obtained by SEC.

ATCC 29213) were selected to screen the activity of our LPs and CPs.

Among terpolymers containing (E) hydrophobic monomer (LPEs: LPE-20 and LPE-30; CPEs: CPE-20 and CPE-30), LPE-20 displayed a MIC_{90} of 32 μg mL^{-1} against *E. coli* (EC K12) and 64–128 μg mL^{-1} against *P. aeruginosa* (PA 27853), while LPE-30 showed enhanced activity with MIC_{90} of 8 μg mL^{-1} (EC K12) and 32 μg mL^{-1} (PA 27853) (Table 2). For the cyclic counterparts, CPE-20 displayed a slightly higher MIC_{90} values of 64 μg mL^{-1} (EC K12) and 256 μg mL^{-1} (PA 27853), whereas CPE-30 exhibited improved potency with MIC_{90} of 16–32 μg mL^{-1} (EC K12) and 128 μg mL^{-1} (PA 27853) (Table 2).

Among the terpolymers containing (P) as the hydrophobic monomer, LPP-30 emerged as the most potent, exhibiting MIC_{90} values of 8–16 μg mL^{-1} against *E. coli* (EC K12) and 16 μg mL^{-1} against *P. aeruginosa* (PA 27853). This was a significant improvement over LPP-20, which showed MIC_{90} values of 32–64 μg mL^{-1} (EC K12) and 256 μg mL^{-1} (PA 27853) (Table 2). Interestingly, CPP-20 was ineffective against both EC K12 and PA 27853 even at the highest tested concentration (256 μg mL^{-1}), while CPP-30 demonstrated a significant improvement in antibacterial activity, with MIC_{90} values of 16–32 μg mL^{-1} (EC K12) and 32–64 μg mL^{-1} (PA 27853) (Table 2). To further confirm these findings, a 3D tomographic microscope was used to visualize a 96-well microplate containing EC K12 treated at MIC_{90} concentrations with LPP-30 and CPP-30. This analysis revealed minimal bacterial growth compared to the untreated control (without polymer), validating the MIC_{90} values obtained (ESI, Fig. S21†). Overall, these results highlight that varying the hydrophobic monomer ratio (20–30%) within the same hydrophobic group can influence MIC_{90} values up to 2–4-fold. Furthermore, terpolymers containing the (P) hydrophobic group generally displayed slightly higher antibacterial activity against *P. aeruginosa* compared to those with the (E) group, with LPP-30 being the most potent overall. Importantly, LPs consistently outperformed their cyclic counterparts against the tested Gram-negative bacteria (Table 2).

Further investigation of antibacterial activity (MIC_{90}) against Gram-positive bacterium (SA 29213) revealed that all our terpolymers, both LPs and CPs, were inactive even at the highest concentration (256 μg mL^{-1}) (Table 2). This finding is consistent with our previous studies using similar type of monomer and composition.[11,73,74] The observed difference in antibacterial activity of the terpolymers against Gram-negative and Gram-positive bacteria can be attributed to their distinctive cell wall structures. Gram-negative bacteria possess a thin, loosely cross-linked peptidoglycan layer covered by an outer membrane with lipopolysaccharides, providing potential anchoring sites for the cationic groups of our polymers.[75] In contrast, Gram-positive cell walls have multiple layers of densely cross-linked peptidoglycan, creating a "sieving effect" that hinders the penetration of bulky hydrophobic molecules.[76,77] The absence of an outer lipopolysaccharide layer, combined with this sieving effect, likely contributes to the inactivity of our terpolymer's against Gram-positive bacteria.[78] Furthermore, Table 2 shows the MIC_{90} values for the control antibiotics, colistin and gentamicin

Table 2 Antibacterial activity of synthetic terpolymers and antibiotics[a]

Polymer or antibacterial drug	MIC$_{90}$, 20 h (μg/mL)				
	E. coli (EC K12)	*P. aeruginosa* (PA 27853)	*S. aureus* (SA 29213)	*A. baumannii* (AB 19606)	*P. aeruginosa* (PA37)
LPE-20	32	64–128	>256	n.d.	n.d.
CPE-20	64	256	>256	n.d.	n.d.
LPE-30	8	32	>256	n.d.	n.d.
CPE-30	16–32	128	>256	n.d.	n.d.
LPP-20	32–64	256	>256	n.d.	n.d.
CPP-20	>256	>256	>256	n.d.	n.d.
LPP-30	8–16	16	>256	16	32–64
CPP-30	16–32	32–64	>256	16–32	128
Colistin	4	4	>256	2–4	4–8
Gentamicin	0.5	0.5	n.d.	8–16	>256
Ciprofloxacin	n.d.	0.12–0.25	n.d.	0.25	16–32

Low MIC$_{90}$ High MIC$_{90}$

[a] Notes: The antibacterial activity of the terpolymers was evaluated by determining the minimum inhibitory concentration (MIC$_{90}$), defined as the lowest concentration required to inhibit 90% of bacterial growth compared to untreated controls after 20 hours of incubation. MIC$_{90}$ values, expressed in μg mL^{-1} of the terpolymers, or antibiotics (colistin, gentamicin, and ciprofloxacin) tested against *E. coli* (EC K12), *P. aeruginosa* (PA 27853), *S. aureus* (SA 29213), *A. baumannii* (AB 19606), and *P. aeruginosa* (PA37, MDR strain). The results are presented in Table 2, with a color scale indicating relative antibacterial efficacy: blue for low MIC$_{90}$ values (high efficacy) and green for high MIC$_{90}$ values (low efficacy). All experiments were performed in triplicate ($n = 3$).

exhibited values of 4 μg mL^{-1} and 0.5 μg mL^{-1}, respectively against *E. coli* (EC K12), while ciprofloxacin demonstrated a range of 0.12 to 0.25 μg mL^{-1} against PA 27853.

Despite our terpolymers exhibiting lower antimicrobial activity compared to conventional antibiotics against standard strains, we expanded our investigation to include two clinically relevant bacterial strains: *A. baumannii* (AB 19606), identified by the WHO as a critical priority pathogen,[6,79] and a multidrug-resistant (MDR) strain of *P. aeruginosa* (PA37). This allowed us to assess the potential of our terpolymers against challenging infections where traditional antibiotics may be less effective or ineffective. We selected our most potent terpolymers, LPP-30 and CPP-30, for further testing against these additional Gram-negative bacteria. Pleasingly, both terpolymers demonstrated good antibacterial activity against AB 19606 and PA37. Specifically, LPP-30 showed MIC$_{90}$ values of 16 μg mL^{-1} and 32–64 μg mL^{-1} against AB 19606 and PA37, respectively, while CPP-30 exhibited MIC$_{90}$ values of 16–32 μg mL^{-1} and 128 μg mL^{-1} against these same strains (Table 2). As a positive control, commercial antibiotic agents were tested, demonstrating expected MIC$_{90}$ values against PA37 and AB 19606 (Table 2). Notably, against MDR strain (PA37), gentamicin was ineffective even at the highest tested concentration (256 μg mL^{-1}), while ciprofloxacin showed significantly reduced efficacy with an MIC$_{90}$ of 16–32 μg mL^{-1}, which is 128-fold increase compared to the PA 27853 (0.12–0.25 μg mL^{-1}). Colistin retained some activity against PA37, but with a lightly higher MIC$_{90}$ value of 4–8 μg mL^{-1}.[80] Overall, PA37 demonstrated slightly lower sensitivity compared to EC K12, PA 27853, and AB 19606. However, the relatively low MIC$_{90}$ values and the smaller fold change in MIC$_{90}$ against PA37, compared to the significant loss of efficacy observed with gentamicin and ciprofloxacin, highlight the promising potential of our terpolymers, particularly LPP-30 and CPP-30, to combat MDR Gram-negative bacterial infections.[73,81]

In all tested different bacterial strains, our LPs exhibited superior antibacterial efficacy compared to their CPs, despite having nearly similar zeta potentials in Milli-Q water (Table 1). Additionally, we observed self-assembly of the terpolymers which may be due to the high concentrations used during DLS analysis (Table 1). However, it is important to note that these assemblies may not form at the lower antibacterial study concentration (Table 2) or disassemble near the bacterial membrane. We attribute this difference in efficacy to the inherent structural properties of LPs. The linear, flexible chains of LPs offer greater conformational freedom, facilitating enhanced mobility and potentially faster diffusion through bacterial membranes compared to the more constrained CPs. Furthermore, the flexibility of LPs allows them to readily adapt upon contact with the bacterial surface, maximizing interactions between their cationic groups and the negatively charged bacterial membrane. This enhanced electrostatic attraction, coupled with hydrophobic interactions between the polymer

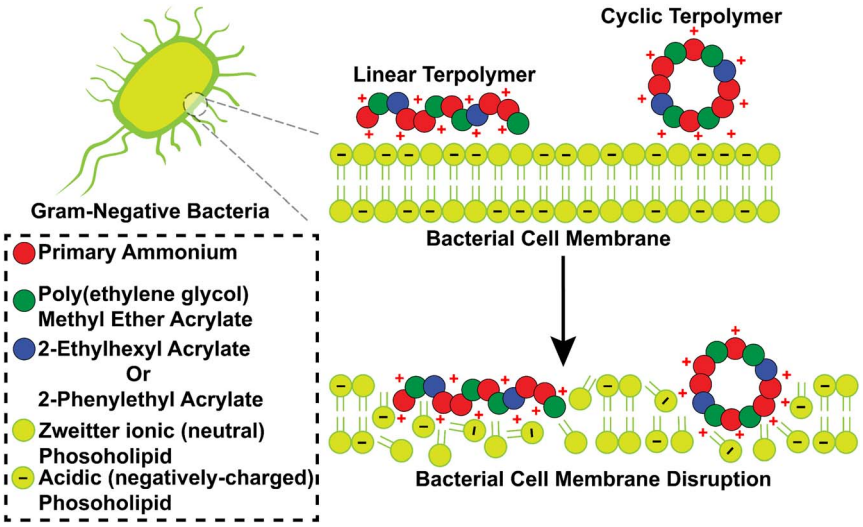

Fig. 3 Proposed mechanism of interaction of cationic linear polymers (LPs) and cyclic polymers (CPs) with Gram-negative bacterial cell membranes. (A) Due to their high flexibility and mobility, LPs can maximize contact with the bacterial membrane, promoting stronger electrostatic interactions and efficient membrane disruption. (B) Conversely, the constrained conformation of CPs limits their surface contact and interaction with the bacterial membrane, potentially reducing their antibacterial activity.

backbone and the phospholipid bilayer, promotes more efficient membrane disruption and ultimately, bacterial cell death (Fig. 3). Conversely, the closed-loop structure of CPs results in more compact structure as noted by DLS in comparison to LPs (Table 1), which limits their flexibility, potentially hindering their interaction with the bacterial membrane (Fig. 3). This reduced molecular mobility could weaken their binding affinity and limit their ability to disrupt the membrane effectively, which is in agreement with a previous study on cyclic glycopolymers.[72]

Cytoplasmic membrane potential study

To validate our hypothesis that CPs and LPs interact differently with bacterial membranes, we conducted a cytoplasmic bacterial membrane (CBM) permeabilization study. Previous studies, including our own, have established that cationic amphiphilic polymers exert their antibacterial effects through membrane disruption *via* electrostatic and hydrophobic interactions.[82–84] Focusing our most potent terpolymers, LPP-30 and CPP-30, we measured the membrane potential of Gram-negative *E. coli* (EC K12) bacteria treated with these polymers. We employed carbocyanine dye 3,3′-diethyloxacarbocyanine iodide, which exhibits red fluorescence when accumulated in bacterial cytosol indicative of intact CBM, but shifts to green fluorescence upon membrane depolarization.[38] By monitoring the red fluorescence intensity (emission at 670 nm), we assessed the extent of membrane disruption. As shown in Fig. 4, LPP-30 induced a greater decrease in red fluorescence intensity compared to CPP-30 terpolymer across a concentration range of 0.0625–1 mg mL^{-1} in a dose-dependent manner after a 5 min incubation. At the lowest concentration tested (0.0625 mg mL^{-1}), the normalized fluorescence intensities of LPP-30 and CPP-30 were approximately 45% and 37%, respectively. This indicates that LPP-30 causes a slightly greater reduction in CBM depolarization than CPP-30, supporting a marginally superior membrane disruption capability for LP.

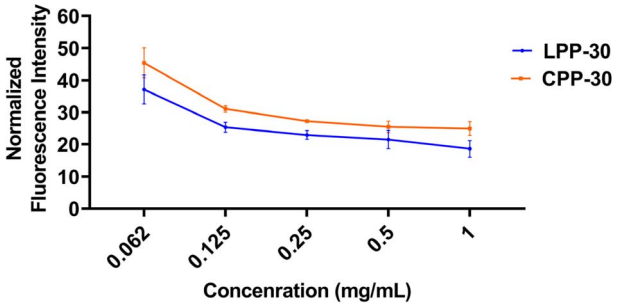

Fig. 4 The red fluorescence (emitting at 670 nm) intensity of Gram-negative, *E. coli* in the presence of different concentrations of LPP-30 and CPP-30 terpolymers.

Bacteria killing study

The bactericidal efficacy of LPP-30 and CPP-30 was further investigated against PA 27853 using a colony forming unit (CFU) assay at different timepoints (15, 30, and 60 minutes) of treatment in a PBS (pH 7.4). Impressively, both terpolymers, at concentrations of 1×MIC (Fig. 5A and B) and 4×MIC (Fig. 5C and D), completely eradicated (99.99%) PA 27853 bacterial cells within the first 15 minutes, resulting in no detectable CFUs compared to the untreated control sample (4.7×10^5 CFU mL^{-1}). Extending the treatment durations to 30 and 60 minutes resulted in complete bacterial killing, highlighting the rapid bactericidal kinetics and potent activity of our terpolymers against PA 27853 (Fig. 5). This rapid bactericidal effect is consistent with previous findings using similar amphiphilic methacrylate copolymers against *E. coli*, where nearly 99.9% of cells were killed within 15–60 minutes at 2×MIC concentrations.[85]

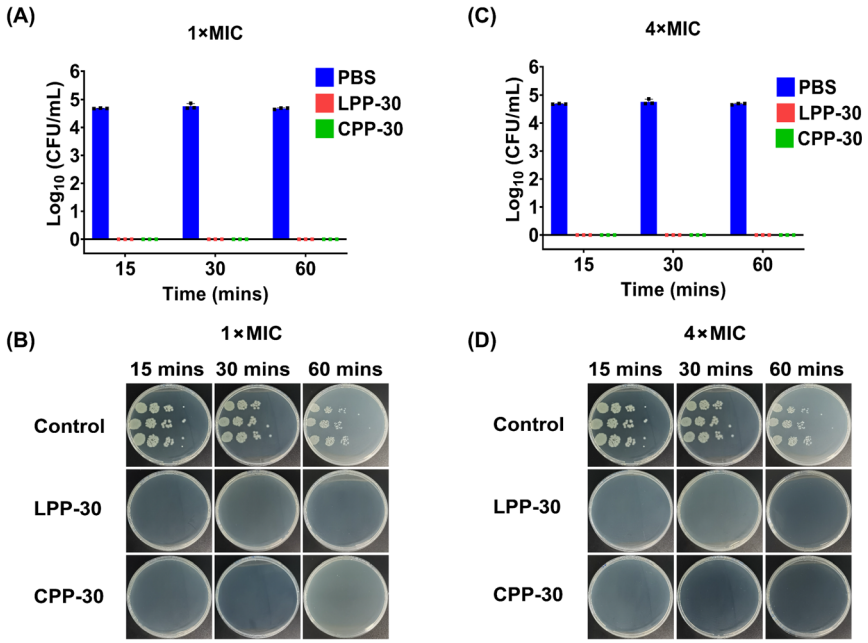

Fig. 5 Time-kill kinetics of LPP-30 and CPP-30 against *P. aeruginosa* PA 27853 cells, determined *via* CFU assay, using an initial concentration of PA 27853 cells of 4.7×10^5 CFU mL^{-1}. The total PA 27853 bacterial cells killed after incubation with different concentration of the terpolymers at 37 °C in PBS (pH 7.4) was plotted against time. Figures (A and B) and (C and D) display the time-kill curves for PA 27853 cells treated with LPP-30 and CPP-30 terpolymers, respectively, at 1×MIC and 4×MIC concentrations for 15, 30, and 60 minutes ($n = 3$). The corresponding MIC_{90} values for LPP-30 and CPP-30 against PA 27853 are provided in Table 2.

Hemolysis and cytotoxicity assay

Given the known cytotoxicity of antimicrobial peptides towards mammalian cells,[23] it is crucial to assess the biocompatibility of our terpolymers. To assess this, we determined the hemolytic activity (HC_{50}) of all terpolymers (LPs and CPs) using defibrinated sheep red blood cells (sRBCs). HC_{50} is defined as the minimum concentration required to induce 50% hemolysis of sRBCs.

Among the terpolymers containing the (E) hydrophobic group, the LPEs (LPE-20 and LPE-30) and CPEs (CPE-20 and CPE-30) displayed distinct hemolytic profiles (Table 3). LPE-20 exhibited HC_{50} values exceeding 1000 μg mL^{-1}, whereas CPE-20 remarkably showed no hemolysis even at the highest tested concentration of 2000 μg mL^{-1}. Increasing the hydrophobic monomer ratio to 30% significantly reduced the HC_{50} values for both LPE-30 and CPE-30 to below 125 μg mL^{-1} (Table 3). For terpolymers containing the (P) hydrophobic group (LPPs and CPPs), LPP-20 showed HC_{50} values above 2000 μg mL^{-1}, a two-fold increase compared to LPE-20 (>1000 μg mL^{-1}) (Table 3). Similar to CPE-20, CPP-20 also showed no hemolytic activity. However, increasing the hydrophobic monomer content to 30% led to a stark contrast in hemolytic behavior. Indeed, LPP-30 was highly hemolytic with HC_{50} below 125 μg mL^{-1}, while CPP-30 maintained excellent hemocompatibility (>2000 μg mL^{-1}), representing a 16-fold improvement over LPP-30 (Table 3). These results demonstrates that while increasing hydrophobicity significantly reduced the HC_{50} values of LP, consistent with previous reports,[11,30,38,78,86] the impact on CPs was less pronounced. This suggests that the cyclic topology, with its reduced flexibility and chain mobility, may confer a degree of protection against hemolysis, even at higher hydrophobic monomer ratios. As APs with complex topologies have been reported to cause hemagglutination,[40,41,47] we decided to conduct a hemagglutination assay, utilizing a previously published protocol.[40] Our results evidenced no hemagglutination at concentrations up to 2000 μg mL^{-1} for all our polymers. Moreover, our control antibiotic, colistin, displayed no hemolytic activity at concentrations up to 2000 μg mL^{-1}. To further assess biocompatibility, we evaluated the cytotoxicity of our terpolymers against the RAW 264.7 cell line using a standard CCK-8 cell viability assay.[83] We determined the minimum concentration required to inhibit cell viability by 50% (IC_{50}, Table 3). Consistent with the hemolysis results, our IC_{50} measurements revealed that CPs (IC_{50} values >64 to >256 μg mL^{-1}) were generally more biocompatible than LPs (IC_{50} values >32 to >128 μg mL^{-1}) (Table 3). This trend aligns with recent findings on the enhanced biocompatibility of cationic cyclic copolymers.[48,50] Furthermore, increasing the hydrophobic content from 20% to 30% in both LPs and CPs led to lower IC_{50} values, consistent with the trend observed in the hemolysis study (Table 3). This suggests that increased hydrophobicity is associated with increased cytotoxicity, regardless of topology. Interestingly, only minor differences in the IC_{50} values between the (E) and (P) hydrophobic monomer groups, indicating that the specific type of hydrophobic monomer had a relatively minor impact on cytotoxicity compared to the overall hydrophobicity level. Lastly, we also assessed the cytotoxicity of common antibiotics: colistin (>128 μg mL^{-1}), gentamicin (>512

Table 3 Summary of hemolytic activity (HC_{50}), cytotoxicity (IC_{50}), PA 27853 (MIC_{90}), and therapeutic index (TI) values of antibacterial terpolymers and antibiotics[a]

Polymer or antibacterial drug	HC_{50}, 2 h (μg/mL)	IC_{50}, 24 h (μg/mL)	*P. aeruginosa* (PA 27853)	Therapeutic Index (HC_{50}/MIC_{90} for PA 27853)	Therapeutic Index (IC_{50}/MIC_{90} for PA 27853)
LPE-20	>1000	>128	64–128	8–15	1–2
CPE-20	No hemolysis	>256	256	>8	1
LPE-30	<125	>32	32	n.d.	1
CPE-30	<125	>128	128	n.d.	1
LPP-20	>2000	n.d.	256	>8	n.d.
CPP-20	No hemolysis	n.d.	>256	n.d.	n.d.
LPP-30	<125	>32	16	n.d.	2
CPP-30	>2000	>64	32–64	31–62	1–2
Colistin	No hemolysis	>128	4	>250	32
Gentamicin	n.d.	>512	0.5	n.d.	>250
Ciprofloxacin	n.d.	>32	0.12–0.25	n.d.	128

Low Hemolysis **High Hemolysis** **Low Cytotoxicity** **High Cytotoxicity**

[a] Notes: (1) The scale shows HC_{50} and IC_{50} values. HC_{50} and IC_{50} values were expressed in μg mL^{-1} of the antibacterial terpolymers and antibiotics. HC_{50} represents the minimum terpolymer concentration causing 50% hemolysis of sheep red blood cells (sRBCs), IC_{50} is defined as the minimum concentration inhibiting 50% of cell viability. The therapeutic index (TI) was calculated by taking the ratio of HC_{50} or IC_{50} and MIC_{90} for *P. aeruginosa* (PA 27853). n.d. not determined. All experiments were conducted in triplicate ($n = 3$). (2) Hemolysis was assessed using a maximum concentration of 2000 μg mL^{-1}. "No hemolysis" indicates no RBC lysis at this concentration. While some hemolysis may have been detected at concentrations exceeding 2000 μg mL^{-1}, the HC_{50} (concentration causing 50% hemolysis) was consistently above this threshold. For therapeutic index (TI) calculations (HC_{50}/MIC_{90} for PA 27853), we conservatively used >2000 μg mL^{-1} as the HC_{50} in all cases.

μg mL^{-1}), and ciprofloxacin (>32 μg mL^{-1}) (Table 3). The obtained cytotoxicity of antibiotics were comparable to other reported studies.[38,87,88]

To evaluate the selectivity of our terpolymers and antibiotics, we calculated their therapeutic index (TI) values, a standard measure of an antibacterial agent's preferential targeting of bacterial cells over mammalian cells.[23] TI values were determined by dividing the HC_{50} or IC_{50} by the MIC_{90} values against PA 27853 (*i.e.*, TI = HC_{50}/MIC_{90} or IC_{50}/MIC_{90}) (Table 3) according to previous published methodologies.[37,71] As shown in Table 3, colistin exhibited a TI value (HC_{50}/MIC_{90}) greater than 250, while the IC_{50}/MIC_{90} values for colistin (32), gentamicin (>250), and ciprofloxacin (128) were higher compared to those of our antibacterial terpolymers (Table 3). Similar TI values for antibiotics have been reported in different antimicrobial polymer studies.[37,41,89] Interestingly the TI (IC_{50}/MIC_{90}) values of both LPs and CPs were comparable, ranging from 1 to 2 (Table 3). However, the calculated TI (HC_{50}/MIC_{90}) value for CP was notably higher than those for LPs. Specifically, CPP-30 showed TI values 31–62, whereas LPE-20 and LPP-20 had TI values of 8–15 and >8, respectively (Table 3).

Taken together, these results highlight the superior biocompatibility and selectivity of CPs compared to LPs. We attribute this difference to the constrained and less flexible nature of CPs, which likely reduces their non-specific interactions with mammalian cell membranes and sRBCs, leading to minimal to no toxicity. Our findings underscore the significant impact of polymer topology and the optimization of hydrophilic/hydrophobic balance in minimizing cytotoxicity and hemolysis and improving TI.

Conclusions

In this study, we successfully synthesized a library of amphiphilic cationic statistical terpolymers with a linear and cyclic topology, designed to mimic the antimicrobial properties of HDPs. The LPs were prepared by RAFT polymerization and subsequently cyclized into CPs *via* a simple and efficient light-induced Diels–Alder click reaction. We systematically investigated the antibacterial properties and biocompatibility of these LPs and CPs, varying the hydrophobic monomer types (E and P) and their content (20–30%). Our results demonstrated that LPs consistently exhibited superior antibacterial activity (MIC_{90}) against 4 Gram-negative bacterial strains compared to their cyclic counterparts. Increasing the hydrophobic content (from 20% to 30%) enhanced their antibacterial activity for both LPs and CPs, and terpolymers containing the (P) hydrophobic group showed slightly superior performance compared to those with the (E) group. Notably, our lead terpolymers, LPP-30 and CPP-30, displayed promising inhibitory effects against the MDR Gram-negative strain *P. aeruginosa* (PA37), outperforming the antibiotics gentamicin and ciprofloxacin. Furthermore,

preliminary mechanistic studies revealed that both LPP-30 and CPP-30 rapidly disrupted bacterial cell membranes, resulting in complete killing of *P. aeruginosa* within 15 minutes. Importantly, CPs exhibited minimal to no hemolytic activity, showcasing a significantly improved safety profile compared to their linear counterparts.

This proof-of-concept study highlights the advantage of tuning polymer topology and optimizing hydrophilic/hydrophobic balance to address the cytotoxicity and selectivity issues associated with HDPs. By systematically exploring the structure–activity relationships of linear *versus* cyclic terpolymers with varying compositions and ratios of hydrophobic monomers, we have provided valuable insights for the rational design of effective and safe APs. These findings pave the way for the development of novel therapeutic strategies to combat the growing threat of antimicrobial resistance.

Data availability

All supporting data is provided in the ESI.†

Author contributions

Conceptualization, methodology, investigation, formal analysis, and writing – original draft: Md.A., methodology, investigation, and validation: W. Y., L. Y., V. K. K., resources, methodology, investigation, and validation: Y. Z., P. L., A. W., C. F., conceptualization, resources, writing – review & editing, and supervision: C. B.

Conflicts of interest

There are no conflicts to declare.

Acknowledgements

Md.A. would like to acknowledge the University International Postgraduate Award (UIPA) from the University of New South Wales (UNSW) for its support. C. B. is the recipient of an Australian Research Council – Australian Laureate Fellowship (project number FL220100016) funded by the Australian Government. C. F. acknowledges the National Health and Medical Research Council for an Investigator Grant (APP1196168). The authors also express their gratitude to Eh Hau Pan, Camillo Taraborrelli, and the NMR facility within the Mark Wainwright Analytical Centre (MWAC) at UNSW for providing technical support and maintaining the necessary instruments. Thanks to Dr Nathaniel Corrigan, Dr Valentin A. Bobrin, Dr Gervase Ng, and Dr Kenny Lee (UNSW) for engaging in many interesting discussions related to chemical and biological experiments. This work used the Queensland node of the NCRIS-enabled Australian National Fabrication Facility (ANFF).

References

1 C. J. Murray, K. S. Ikuta, F. Sharara, L. Swetschinski, G. R. Aguilar, A. Gray, C. Han, C. Bisignano, P. Rao and E. Wool, Global burden of bacterial antimicrobial resistance in 2019: a systematic analysis, *Lancet*, 2022, **399**, 629–655.
2 *10 global health issues to track in 2021*, **https://www.who.int/news-room/spotlight/10-global-health-issues-to-track-in-2021**, (accessed 09 July, 2024).
3 *Antimicrobial resistance*, **https://www.who.int/news-room/fact-sheets/detail/antimicrobial-resistance** (accessed 09 July 2024).
4 *Antimicrobial resistance: a silent pandemic*, Nature Communications, 2024, vol. 15, p. 6198, **https://www.nature.com/articles/s41467-024-50457-z**.
5 *WHO reports widespread overuse of antibiotics in patients hospitalized with COVID-19*, **https://www.who.int/news/item/26-04-2024-who-reports-widespread-overuse-of-antibiotics-in-patients–hospitalized-with-covid-19**, (accessed 09 July, 2024).
6 C. Willyard, Drug-resistant bacteria ranked, *Nature*, 2017, **543**, 15.
7 W. H. Organization, *Global antimicrobial resistance and use surveillance system (GLASS) report 2022*, World Health Organization, 2022.
8 W. H. Organization, *2021 antibacterial agents in clinical and preclinical development: an overview and analysis*, 2022.
9 J. O'Neill, *Tackling drug-resistant infections globally: final report and recommendations*, 2016.
10 P. Pham, S. Oliver and C. Boyer, Design of antimicrobial polymers, *Macromol. Chem. Phys.*, 2023, **224**, 2200226.
11 P. T. Phuong, S. Oliver, J. He, E. H. Wong, R. T. Mathers and C. Boyer, Effect of hydrophobic groups on antimicrobial and hemolytic activity: Developing a predictive tool for ternary antimicrobial polymers, *Biomacromolecules*, 2020, **21**, 5241–5255.
12 H. Takahashi, G. A. Caputo, S. Vemparala and K. Kuroda, Synthetic random copolymers as a molecular platform to mimic host-defense antimicrobial peptides, *Bioconjugate Chem.*, 2017, **28**, 1340–1350.
13 A. Jain, L. S. Duvvuri, S. Farah, N. Beyth, A. J. Domb and W. Khan, Antimicrobial polymers, *Adv. Healthcare Mater.*, 2014, **3**, 1969–1985.
14 R. E. Hancock and H.-G. Sahl, Antimicrobial and host-defense peptides as new anti-infective therapeutic strategies, *Nat. Biotechnol.*, 2006, **24**, 1551–1557.
15 A. G. Elliott, J. X. Huang, S. Neve, J. Zuegg, I. A. Edwards, A. K. Cain, C. J. Boinett, L. Barquist, C. V. Lundberg and J. Steen, An amphipathic peptide with antibiotic activity against multidrug-resistant Gram-negative bacteria, *Nat. Commun.*, 2020, **11**, 3184.
16 R. W. Scott, W. F. DeGrado and G. N. Tew, De novo designed synthetic mimics of antimicrobial peptides, *Curr. Opin. Biotechnol.*, 2008, **19**, 620–627.
17 Z. Si, W. Zheng, D. Prananty, J. Li, C. H. Koh, E.-T. Kang, K. Pethe and M. B. Chan-Park, Polymers as advanced antibacterial and antibiofilm agents for direct and combination therapies, *Chem. Sci.*, 2022, **13**, 345–364.
18 G. J. Gabriel, J. A. Maegerlein, C. F. Nelson, J. M. Dabkowski, T. Eren, K. Nüsslein and G. N. Tew, Comparison of facially

amphiphilic versus segregated monomers in the design of antibacterial copolymers, *Chem.–A Euro. J.*, 2009, **15**, 433–439.

19 H. Takahashi, I. Sovadinova, K. Yasuhara, S. Vemparala, G. A. Caputo and K. Kuroda, Biomimetic antimicrobial polymers—Design, characterization, antimicrobial, and novel applications, *Wiley Interdiscip. Rev.: Nanomed. Nanobiotechnol.*, 2023, **15**, e1866.

20 M. Zasloff, Antimicrobial peptides of multicellular organisms, *nature*, 2002, **415**, 389–395.

21 H. Takahashi, G. A. Caputo and K. Kuroda, Amphiphilic polymer therapeutics: An alternative platform in the fight against antibiotic resistant bacteria, *Biomater. Sci.*, 2021, **9**, 2758–2767.

22 E. F. Palermo and K. Kuroda, Structural determinants of antimicrobial activity in polymers which mimic host defense peptides, *Appl. Microbiol. Biotechnol.*, 2010, **87**, 1605–1615.

23 Z. Shao, K. Hakobyan, J. Xu, R. Chen, N. Kumar, M. Willcox and E. H. Wong, Photoinduced Unveiling of Cationic Amine: Toward Smart Photoresponsive Antimicrobial Polymers, *ACS Appl. Polym. Mater.*, 2023, **5**, 8735–8743.

24 P. Askari, M. H. Namaei, K. Ghazvini and M. Hosseini, In vitro and in vivo toxicity and antibacterial efficacy of melittin against clinical extensively drug-resistant bacteria, *BMC Pharmacol. Toxicol.*, 2021, **22**, 1–12.

25 Y. Geng, Y. Yuan, Y. Bao, S. Huang, X. Wang, L. Huang, C. She, X. Gong and M. Xiong, pH window for high selectivity of ionizable antimicrobial polymers toward bacteria, *ACS Appl. Mater. Interfaces*, 2023, **15**, 21781–21791.

26 J. Tan, Y. Zhao, J. L. Hedrick and Y. Y. Yang, Effects of Hydrophobicity on Antimicrobial Activity, Selectivity, and Functional Mechanism of Guanidinium-Functionalized Polymers, *Adv. Healthcare Mater.*, 2022, **11**, 2100482.

27 E. F. Palermo and K. Kuroda, Chemical structure of cationic groups in amphiphilic polymethacrylates modulates the antimicrobial and hemolytic activities, *Biomacromolecules*, 2009, **10**, 1416–1428.

28 A. Kuroki, A. K. Tchoupa, M. Hartlieb, R. Peltier, K. E. Locock, M. Unnikrishnan and S. Perrier, Targeting intracellular, multi-drug resistant Staphylococcus aureus with guanidinium polymers by elucidating the structure-activity relationship, *Biomaterials*, 2019, **217**, 119249.

29 B. P. Mowery, A. H. Lindner, B. Weisblum, S. S. Stahl and S. H. Gellman, Structure– activity relationships among random nylon-3 copolymers that mimic antibacterial host-defense peptides, *J. Am. Chem. Soc.*, 2009, **131**, 9735–9745.

30 K. Kuroda and W. F. DeGrado, Amphiphilic polymethacrylate derivatives as antimicrobial agents, *J. Am. Chem. Soc.*, 2005, **127**, 4128–4129.

31 P. R. Judzewitsch, T. K. Nguyen, S. Shanmugam, E. H. Wong and C. Boyer, Towards sequence-controlled antimicrobial polymers: effect of polymer block order on antimicrobial activity, *Angew. Chem., Int. Ed.*, 2018, **57**, 4559–4564.

32 S. Venkataraman, J. P. Tan, S. T. Chong, C. Y. Chu, E. A. Wilianto, C. X. Cheng and Y. Y. Yang, Identification of structural attributes contributing to the potency and selectivity of antimicrobial polyionenes: Amides are better than esters, *Biomacromolecules*, 2019, **20**, 2737–2742.

33 P. R. Judzewitsch, N. Corrigan, F. Trujillo, J. Xu, G. Moad, C. J. Hawker, E. H. Wong and C. Boyer, High-throughput process for the discovery of antimicrobial polymers and their upscaled production via flow polymerization, *Macromolecules*, 2020, **53**, 631–639.

34 A. Kuroki, P. Sangwan, Y. Qu, R. Peltier, C. Sanchez-Cano, J. Moat, C. G. Dowson, E. G. Williams, K. E. Locock and M. Hartlieb, Sequence control as a powerful tool for improving the selectivity of antimicrobial polymers, *ACS Appl. Mater. Interfaces*, 2017, **9**, 40117–40126.

35 P. Gurnani, T. Floyd, J. Tanaka, C. Stubbs, D. Lester, C. Sanchez-Cano and S. Perrier, PCR-RAFT: rapid high throughput oxygen tolerant RAFT polymer synthesis in a biology laboratory, *Polym. Chem.*, 2020, **11**, 1230–1236.

36 N. Corrigan, K. Jung, G. Moad, C. J. Hawker, K. Matyjaszewski and C. Boyer, Reversible-deactivation radical polymerization (Controlled/living radical polymerization): From discovery to materials design and applications, *Prog. Polym. Sci.*, 2020, **111**, 101311.

37 M. Aquib, S. Schaefer, H. Gmedhin, N. Corrigan, V. A. Bobrin and C. Boyer, Shape matters: Effect of amphiphilic polymer topology on antibacterial activity and hemocompatibility, *Eur. Polym. J.*, 2024, **205**, 112698.

38 T.-K. Nguyen, S. J. Lam, K. K. Ho, N. Kumar, G. G. Qiao, S. Egan, C. Boyer and E. H. Wong, Rational design of single-chain polymeric nanoparticles that kill planktonic and biofilm bacteria, *ACS Infect. Dis.*, 2017, **3**, 237–248.

39 S. Y. Nam, J. Lee, S. S. Shin, H. J. Yoo, M. Yun, S. Kim, J. H. Kim and J.-H. Lee, Antibacterial and cytotoxic properties of star-shaped quaternary ammonium-functionalized polymers with different pendant groups, *Polym. Chem.*, 2022, **13**, 1763–1773.

40 R. Namivandi-Zangeneh, R. J. Kwan, T.-K. Nguyen, J. Yeow, F. L. Byrne, S. H. Oehlers, E. H. Wong and C. Boyer, The effects of polymer topology and chain length on the antimicrobial activity and hemocompatibility of amphiphilic ternary copolymers, *Polym. Chem.*, 2018, **9**, 1735–1744.

41 S. Schaefer, D. Melodia, N. Corrigan, M. D. Lenardon and C. Boyer, Effect of star topology versus linear polymers on antifungal activity and mammalian cell toxicity, *Macromol. Biosci.*, 2024, **24**, 2300452.

42 S. Laroque, M. Reifarth, M. Sperling, S. Kersting, S. Klöpzig, P. Budach, J. Storsberg and M. Hartlieb, Impact of multivalence and self-assembly in the design of polymeric antimicrobial peptide mimics, *ACS Appl. Mater. Interfaces*, 2020, **12**, 30052–30065.

43 A.-C. Lehnen, A. M. Bapolisi, M. Krass, A. AlSawaf, J. Kurki, S. Kersting, H. Fuchs and M. Hartlieb, Shape matters: Highly selective Antimicrobial Bottle Brush copolymers via a one-pot RAFT polymerization approach, *Biomacromolecules*, 2022, **23**, 5350–5360.

44 A. C. Lehnen, S. Kogikoski Jr, T. Stensitzki, A. AlSawaf, A. M. Bapolisi, M. Wolff, J. De Breuck, H. M. Müller-Werkmeister, S. Chiantia and I. Bald,

Anisotropy in Antimicrobial Bottle Brush Copolymers and Its Influence on Biological Activity, *Adv. Funct. Mater.*, 2024, **34**, 2312651.

45 S. J. Lam, N. M. O'Brien-Simpson, N. Pantarat, A. Sulistio, E. H. Wong, Y.-Y. Chen, J. C. Lenzo, J. A. Holden, A. Blencowe and E. C. Reynolds, Combating multidrug-resistant Gram-negative bacteria with structurally nanoengineered antimicrobial peptide polymers, *Nat. Microbiol.*, 2016, **1**, 1–11.

46 S. J. Lam, E. H. Wong, N. M. O'Brien-Simpson, N. Pantarat, A. Blencowe, E. C. Reynolds and G. G. Qiao, Bionano interaction study on antimicrobial star-shaped peptide polymer nanoparticles, *ACS Appl. Mater. Interfaces*, 2016, **8**, 33446–33456.

47 S. Laroque, R. n. Garcia Maset, A. Hapeshi, F. Burgevin, K. E. Locock and S. Perrier, Synthetic star nanoengineered antimicrobial polymers as antibiofilm agents: Bacterial membrane disruption and cell aggregation, *Biomacromolecules*, 2023, **24**, 3073–3085.

48 J. Xu, L. Pu, J. Ma, S. K. Kumar and H. Duan, Antibacterial properties of synthesized cyclic and linear cationic copolymers, *Polym. Chem.*, 2020, **11**, 6632–6639.

49 M. Porel, D. N. Thornlow, N. N. Phan and C. A. Alabi, Sequence-defined bioactive macrocycles via an acid-catalysed cascade reaction, *Nat. Chem.*, 2016, **8**, 590–596.

50 P. Salas-Ambrosio, A. Tronnet, M. Since, S. Bourgeade-Delmas, J.-L. Stigliani, A. Vax, S. Lecommandoux, B. Dupuy, P. Verhaeghe and C. Bonduelle, Cyclic poly (α-peptoid) s by lithium bis (trimethylsilyl) amide (LiHMDS)-mediated ring-expansion polymerization: simple access to bioactive backbones, *J. Am. Chem. Soc.*, 2021, **143**, 3697–3702.

51 B. P. Mowery, S. E. Lee, D. A. Kissounko, R. F. Epand, R. M. Epand, B. Weisblum, S. S. Stahl and S. H. Gellman, Mimicry of antimicrobial host-defense peptides by random copolymers, *J. Am. Chem. Soc.*, 2007, **129**, 15474–15476.

52 Z. Jia and M. J. Monteiro, Cyclic polymers: Methods and strategies, *J. Polym. Sci., Part A: Polym. Chem.*, 2012, **50**, 2085–2097.

53 C. Chen and T. Weil, Cyclic polymers: synthesis, characteristics, and emerging applications, *Nanoscale Horiz.*, 2022, **7**, 1121–1135.

54 J. Pribyl, E. Sullivan, A. Nadeem and S. Grayson, Photoiniferter Synthesis of Cyclic Polymers from Vinyl Monomers, *Macromolecules*, 2024, **57**, 7556–7564.

55 F. M. Haque and S. M. Grayson, The synthesis, properties and potential applications of cyclic polymers, *Nat. Chem.*, 2020, **12**, 433–444.

56 B. Golba, E. M. Benetti and B. G. De Geest, Biomaterials applications of cyclic polymers, *Biomaterials*, 2021, **267**, 120468.

57 H. R. Kricheldorf, Cyclic polymers: Synthetic strategies and physical properties, *J. Polym. Sci., Part A: Polym. Chem.*, 2010, **48**, 251–284.

58 J. N. Hoskins and S. M. Grayson, Synthesis and degradation behavior of cyclic poly (ε-caprolactone), *Macromolecules*, 2009, **42**, 6406–6413.

59 R. J. Williams, A. P. Dove and R. K. O'Reilly, Self-assembly of cyclic polymers, *Polym. Chem.*, 2015, **6**, 2998–3008.

60 B. Chen, K. Jerger, J. M. Fréchet and F. C. Szoka Jr, The influence of polymer topology on pharmacokinetics: differences between cyclic and linear PEGylated poly (acrylic acid) comb polymers, *J. Controlled Release*, 2009, **140**, 203–209.

61 G. Kang, L. Sun, Y. Liu, C. Meng, W. Ma, B. Wang, L. Ma, C. Yu and H. Wei, Micelles with cyclic poly (ε-caprolactone) moieties: greater stability, larger drug loading capacity, and slower degradation property for controlled drug release, *Langmuir*, 2019, **35**, 12509–12517.

62 R. Liénard, J. De Winter and O. Coulembier, Cyclic polymers: Advances in their synthesis, properties, and biomedical applications, *J. Polym. Sci.*, 2020, **58**, 1481–1502.

63 T. Josse, O. Altintas, K. K. Oehlenschlaeger, P. Dubois, P. Gerbaux, O. Coulembier and C. Barner-Kowollik, Ambient temperature catalyst-free light-induced preparation of macrocyclic aliphatic polyesters, *Chem. Commun.*, 2014, **50**, 2024–2026.

64 K. K. Oehlenschlaeger, J. O. Mueller, N. B. Heine, M. Glassner, N. K. Guimard, G. Delaittre, F. G. Schmidt and C. Barner-Kowollik, Light-induced modular ligation of conventional RAFT polymers, *Angew. Chem., Int. Ed.*, 2013, **52**, 762–766.

65 T. Pauloehrl, G. Delaittre, V. Winkler, A. Welle, M. Bruns, H. G. Börner, A. M. Greiner, M. Bastmeyer and C. Barner-Kowollik, Adding spatial control to click chemistry: phototriggered Diels–Alder surface (bio) functionalization at ambient temperature, *Angew. Chem., Int. Ed.*, 2012, **51**, 1071–1074.

66 M. Glassner, K. K. Oehlenschlaeger, T. Gruendling and C. Barner-Kowollik, Ambient temperature synthesis of triblock copolymers via orthogonal photochemically and thermally induced modular conjugation, *Macromolecules*, 2011, **44**, 4681–4689.

67 T. Gruendling, K. K. Oehlenschlaeger, E. Frick, M. Glassner, C. Schmid and C. Barner-Kowollik, Rapid UV Light-Triggered Macromolecular Click Conjugations via the Use of o-Quinodimethanes, *Macromol. Rapid Commun.*, 2011, **32**, 807–812.

68 Q. Tang, Y. Wu, P. Sun, Y. Chen and K. Zhang, Powerful ring-closure method for preparing varied cyclic polymers, *Macromolecules*, 2014, **47**, 3775–3781.

69 P. Sun, Z. Zhang and K. Zhang, Scalable preparation of cyclic polymers by the ring-closure method assisted by the continuous-flow technique, *Polym. Chem.*, 2016, **7**, 2239–2244.

70 Q. Li, T. Dong, X. Liu and X. Lei, A bioorthogonal ligation enabled by click cycloaddition of o-quinolinone quinone methide and vinyl thioether, *J. Am. Chem. Soc.*, 2013, **135**, 4996–4999.

71 S. Schaefer, T. T. P. Pham, S. Brunke, B. Hube, K. Jung, M. D. Lenardon and C. Boyer, Rational design of an antifungal polyacrylamide library with reduced host-cell toxicity, *ACS Appl. Mater. Interfaces*, 2021, **13**, 27430–27444.

72 M. Nagao, Y. Hoshino and Y. Miura, Synthesis of well-defined cyclic glycopolymers and the relationship between their physical properties and their interaction with lectins, *Polym. Chem.*, 2022, **13**, 5453–5457.
73 P. Pham, S. Oliver, E. H. Wong and C. Boyer, Effect of hydrophilic groups on the bioactivity of antimicrobial polymers, *Polym. Chem.*, 2021, **12**, 5689–5703.
74 P. R. Judzewitsch, L. Zhao, E. H. Wong and C. Boyer, High-throughput synthesis of antimicrobial copolymers and rapid evaluation of their bioactivity, *Macromolecules*, 2019, **52**, 3975–3986.
75 H. I. Zgurskaya, C. A. López and S. Gnanakaran, Permeability barrier of Gram-negative cell envelopes and approaches to bypass it, *ACS Infect. Dis.*, 2015, **1**, 512–522.
76 K. Lienkamp, K. N. Kumar, A. Som, K. Nüsslein and G. N. Tew, "Doubly selective" antimicrobial polymers: how do they differentiate between bacteria?, *Chem.–A Euro. J.*, 2009, **15**, 11710–11714.
77 W. Chin, C. Yang, V. W. L. Ng, Y. Huang, J. Cheng, Y. W. Tong, D. J. Coady, W. Fan, J. L. Hedrick and Y. Y. Yang, Biodegradable broad-spectrum antimicrobial polycarbonates: Investigating the role of chemical structure on activity and selectivity, *Macromolecules*, 2013, **46**, 8797–8807.
78 P. Pham, S. Oliver, D. T. Nguyen and C. Boyer, Effect of Cationic Groups on the Selectivity of Ternary Antimicrobial Polymers, *Macromol. Rapid Commun.*, 2022, **43**, 2200377.
79 L. Dijkshoorn, A. Nemec and H. Seifert, An increasing threat in hospitals: multidrug-resistant Acinetobacter baumannii, *Nat. Rev. Microbiol.*, 2007, **5**, 939–951.
80 K. LaPlante, J. Cusumano and G. Tillotson, Colistin for the treatment of multidrug-resistant infections, *Lancet Infect. Dis.*, 2018, **18**, 1174–1175.
81 Z. Pang, R. Raudonis, B. R. Glick, T.-J. Lin and Z. Cheng, Antibiotic resistance in Pseudomonas aeruginosa: mechanisms and alternative therapeutic strategies, *Biotechnol. Adv.*, 2019, **37**, 177–192.
82 M. Tsukamoto, E. Zappala, G. A. Caputo, J.-i. Kikuchi, K. Najarian, K. Kuroda and K. Yasuhara, Mechanistic study of membrane disruption by antimicrobial methacrylate random copolymers by the single giant vesicle method, *Langmuir*, 2021, **37**, 9982–9995.
83 Y. Gong, X. Xu, M. Aquib, Y. Zhang, W. Yang, Y. Chang, H. Peng, C. Boyer, A. K. Whittaker and C. Fu, Ammonium, Phosphonium, and Sulfonium Polymers for Antimicrobial Applications: A Comparative Study, *ACS Appl. Polym. Mater.*, 2024, **6**, 6966–6975.
84 T. Zhang, W. An, J. Sun, F. Duan, Z. Shao, F. Zhang, T. Jiang, X. Deng, C. Boyer and W. Gao, N-terminal lysozyme conjugation to a cationic polymer enhances antimicrobial activity and overcomes antimicrobial resistance, *Nano Lett.*, 2022, **22**, 8294–8303.
85 E. F. Palermo, S. Vemparala and K. Kuroda, Cationic spacer arm design strategy for control of antimicrobial activity and conformation of amphiphilic methacrylate random copolymers, *Biomacromolecules*, 2012, **13**, 1632–1641.
86 K. Kuroda, G. A. Caputo and W. F. DeGrado, The role of hydrophobicity in the antimicrobial and hemolytic activities of polymethacrylate derivatives, *Chem.–A Euro. J.*, 2009, **15**, 1123–1133.
87 Z. Shao, E. Wulandari, R. C. Lin, J. Xu, K. Liang and E. H. Wong, Two plus one: combination therapy tri-systems involving two membrane-disrupting antimicrobial macromolecules and antibiotics, *ACS Infect. Dis.*, 2022, **8**, 1480–1490.
88 A. Kovacik, E. Tvrda, T. Jambor, D. Fulopova, E. Kovacikova, L. Hleba, Ł. M. Kołodziejczyk, M. Hlebova, A. Gren and P. Massanyi, Cytotoxic effect of aminoglycoside antibiotics on the mammalian cell lines, *J. Environ. Sci. Health, Part A: Toxic/Hazard. Subst. Environ. Eng.*, 2020, **56**, 1–8.
89 Z. Y. Ong, S. J. Gao and Y. Y. Yang, Short synthetic β-sheet forming peptide amphiphiles as broad spectrum antimicrobials with antibiofilm and endotoxin neutralizing capabilities, *Adv. Funct. Mater.*, 2013, **23**, 3682–3692.